Bimetallic Ni-Co nanoparticles as an efficient catalyst of hydrogen generation via hydrolysis of NaBH4

A. Kytsya [a,b], V. Berezovets [a], Yu. Verbovytskyy [a], L. Bazylyak [b], V. Kordan [c], I. Zavaliy [a,*], V.A. Yartys [d,*]

[a] Karpenko Physico-Mechanical Institute NAS of Ukraine, 5 Naukova Str., Lviv 79060, Ukraine
[b] Department of Physical Chemistry of Fossil Fuels of the Institute of Physical-Organic Chemistry and Coal Chemistry named after L. M. Lytvynenko of the National Academy of Sciences of Ukraine, 3a Naukova Str., Lviv 79060, Ukraine
[c] Ivan Franko Lviv National University, Kyryla and Mefodija Str. 6, Lviv 79000, Ukraine
[d] Institute for Energy Technology, P.O. Box 40, N-2027 Kjeller, Norway

ARTICLE INFO

ABSTRACT

Ni-Co bimetallic nanoparticles (NPs) have been synthesized via reduction of Ni and Co hydroxides by hydrazine in water / ethylene glycol solutions. It was found that the particle size and polydispersity of the obtained chemically homogeneous NPs decrease with a decreasing to 50 at.% content of Ni in the reaction mixture. A different trend was observed for $Ni_{25}Co_{75}$ and was related to the formation of Ni- and Co-rich particles. Ni-Co-NPs were tested as catalysts of hydrolysis of alkaline solutions of $NaBH_4$, with the highest rate of hydrogen generation observed for $Ni_{50}Co_{50}$. Zero-order kinetics of hydrogen evolution process was observed for all studied systems. Based on the data of the kinetic studies, we conclude that the rate of the hydrolysis process (a) increased with increasing $NaBH_4$ concentration in the range 0.1 – 1 mol/L; (b) decreased by 25% with increasing pH of the solution from 9 to 14. Studies of the temperature dependence of the rates of the hydrolysis process showed that the activation energy of the reaction decreased to 26 kJ/mol with decreasing contents of $NaBH_4$ and catalysts. Based on a comparison of the values of activation energy of hydrolysis reaction and the enthalpy of activation of viscous flow of initial $NaBH_4$ solution and the solution obtained after the hydrolysis, a diffusion-controlled reaction mechanism was proposed.

© 2022 The Author(s). Published by Elsevier B.V.
CC_BY_4.0

1. Introduction

Sodium borohydride ($NaBH_4$) is a well-studied material for hydrogen generation and storage. It provides such practical advantages as high gravimetric hydrogen storage capacity (10.8 wt% H), chemical stability, non-flammability at room temperature, and recyclability of the byproduct of its hydrolysis. High costs of $NaBH_4$ and difficult recycling of the byproducts are the main drawbacks which make impossible a utilization of such a material for hydrogen supply in the large-scale practical applications. Nevertheless, recently developed [1,2] low-cost regeneration method of $Na(Li)BH_4$ by-products mitigates these shortcomings and the requirements for the commercial applications can be met. Recently the US Department of Energy terminated the R&D activities on the use of the solutions of sodium borohydride for hydrogen supply as a fuel for on-board

vehicular applications. Nevertheless, for hydrogen supply for the portable energy generation, when the amount of $NaBH_4$ used is modest/small while the regeneration of the by-products is not so important, an interest to the use of $NaBH_4$ remains high. As an example, a portable 30 W power supply system was successfully developed by the authors while utilizing aqueous solution of $NaBH_4$ as a hydrogen generation material [3].

A catalyzed hydrolysis of $NaBH_4$ generates a large amount of hydrogen via the following process:

$$NaBH_4 + (2+x)\,H_2O = NaBO_2 \cdot xH_2O + 4\,H_2.$$
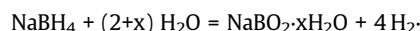
Over the last two decades, various aspects of $NaBH_4$ hydrolysis have been studied in detail. The data of such studies are summarized and discussed in the review papers [4–12]. One focus of such research is related to the synthesis and studies of the efficient catalysts aimed to improve and control hydrolysis of $NaBH_4$. Heterogeneous catalysts exhibit superior catalytic activity towards the hydrolysis of $NaBH_4$ and provide high hydrogen generation rates (HGR). As high cost and limited supply usually restrain large-scale applications of

---

* Corresponding authors.
  E-mail addresses: ihor.zavaliy@gmail.com (I. Zavaliy), volodymyr.yartys@ife.no (V.A. Yartys).

noble metals, development of low-cost and highly efficient catalysts is in high demand. Thus, besides the noble metals, cost-efficient bi- and multi-metal catalysts based on transition metals Co and Ni attract great attention. Indeed, several dozens of reference works describe studies of Co-Ni based catalysts [13–39].

Catalytic activity of the Ni-Co based catalysts obtained by the chemical reduction processes is described in [15,16,18,19,21,22, 33,37,39]. The Co-Ni-B catalysts were mainly obtained by using $NaBH_4$ as a reducing agent in a vigorously stirred mixed solution of $NiCl_2$ and $CoCl_2$. Fernanders et al. [16,18,19] studied Ni-Co-B and Ni-Co-P-B catalysts and selected the most efficient one with the (Co/Co + Ni) molar ratio of 0.85. The highest HGR and the lowest activation energy of the process (E_A) were found to be 2400 mL/min/g and 29 kJ/mol. The Co-Ni-B based catalyst [37] containing crystalline CoB and Ni_4B_3 exhibited the highest H_2 generation rate (500 mL/min/g) with apparent activation energy of 32.7 kJ/mol.

Studies of the hydrogen generation from alkaline $NaBH_4$ solution using Ni-Co based catalysts synthesized by electroless deposition were performed in [20,23,26–30]. TiO_2, Al_2O_3, graphene oxide or Cu sheet were used as the carriers. Hydrogen generation from catalytic hydrolysis of a sodium borohydride solution using supported amorphous alloy catalysts including Ni-Co-P/γ-Al_2O_3, Co-Ni-Mo-P/γ-Al_2O_3, and Co-Ni-W-P/γ-Al_2O_3 was studied in [26,28,30]. HGR and E_A of 6599.6 (T = 55 ºC) and 52.05, 13,842 (T = 45 ºC) and 52.43, 5600 mL/min/g (T = 45 ºC) and 49.19 kJ/mol, respectively, were reported. The highest hydrogen evolution rate for $NaBH_4$ hydrolysis of 14,778 mL/min/g and the activation energy of 42.8 kJ/mol were obtained by Wei et al. [29] using nanostructured Co-Ni-B catalysts deposited on Cu sheet. Hydrothermal deposition and phosphating methods for preparing catalysts in a form of NiCoP nanosheet array on Ti mesh and 3D urchin on Ni foam were studied in [31,34]. Electrodeposition method was applied in [17,24,25,35,36] to prepare different Ni-Co catalysts on Cu sheet or Ni foam supports. Solutions of Ni^{2+} and Co^{2+} salts (chlorides, nitrates, sulfates or sulfamates) were used as the metal sources. Phosphorus containing catalysts Co-Ni-P/Cu [24] and Ni-Co_x-P @ Ni (x = 20) [37] are characterized by high hydrogen generation rates (3636 and 4323 mL/min/g) and the low activation energies (38 and 30 kJ/mol), which are comparable to the performances of the noble metals.

Boron-free catalysts were studied in [13,14]. The filamentary Ni mixed Co catalyst ($Ni_{20}Co_{80}$) consolidated by styrene-butadiene-rubber showed a maximum hydrogen production rate of 96.3 mL/ min/g [13]. Catalytic properties of Raney Ni-Co powder [14] prepared from the alloys of nickel and cobalt showed an increased activity as compared to the pure metals. The $Ni_{50}Co_{50}$ catalyst exhibits HGR of 648.2 mL/min/g and E_A of 52.5 kJ/mol. Low cost and advanced performance make them promising candidates as the catalysts of hydrogen generation from the sodium borohydride.

In this study, we synthesized binary Ni-Co nanoparticles by a chemical reduction of a mixture of nickel and cobalt hydroxides using hydrazine. The produced catalysts of hydrogen generation from borohydride were characterized by SEM and XRD analyses. Factors influencing hydrogen generation rate such as Ni/Co ratio, reagent concentration, pH, and temperature were studied. Efficiencies of various catalysts are compared, and the most efficient catalysts are proposed.

2. Experimental details

2.1. Synthesis and characterization of the catalyst

Bimetallic Ni-Co nanoparticles (Ni-Co-NPs) were synthesized via a reduction of a freshly prepared mixture of nickel and cobalt hydroxides by hydrazine in water / ethylene glycol (EG) solutions at 70 °C. Nickel acetate (Ni($CH_3COO)_2$ × 4 H_2O, Sfera Sim, Ukraine, > 99.5%) and cobalt acetate (Co($CH_3COO)_2$ × 4 H_2O, Sfera

Sim, Ukraine, > 99.5%) were dissolved in EG (Sfera Sim, Ukraine, > 99%), and the water solution of NaOH (titrant, Kharkovreachem, Ukraine) was added under continuous stirring. After reaching the operating temperature, an excess of hydrazine (N_2H_4 ×H_2O, Sfera Sim, Ukraine, > 99%) was added and the reaction mixture was rigorously stirred for 20 – 40 min until a gas evolution was completed. Obtained black precipitate was separated from the supernatant using external magnetic field, washed by deionized water, and stored under the water. The supernatant was tested using UV–vis spectroscopy (Shimadzu UV-mini 1240). The obtained spectra did not contain any extra peaks as compared to the reference solution. This confirmed a full conversion of the precursors into the target products. We note that the reduction of Co($OH)_2$ to metallic cobalt does not occur at the studied experimental conditions. The data on the kinetics and mechanism of the formation of Ni-Co-NPs will be presented elsewhere.

Phase-structural analysis of the samples was carried out by X-ray powder diffraction (XRD) using DRON 3 M diffractometer (Fe-Kα radiation). The collected XRD data were processed by Rietveld profile refinement method using FullProf software [40]. Morphology and elemental composition of Ni-Co-NPs were examined by scanning electron microscopy (SEM) using a Carl Zeiss EVO 40XVP microscope equipped with Inca Energy 350 spectrometer for energy dispersive X-ray analysis (EDS) and a Tescan Vega 3 LMU microscope.

2.2. Characterization of the hydrolysis process

Kinetics of hydrolysis of $NaBH_4$ was studied at pseudo-isothermal conditions in a setup similar to that described in [41,42] and consisting of a two-neck glass vessel immersed into a thermostated water bath (accuracy of temperature maintenance was 0.2 °C) equipped with a magnetic stirrer and injector of the solution of $NaBH_4$. Typically, 0.3 g of a catalyst was added to a 5 mL of alkaline aqueous solution of $NaBH_4$. The generated hydrogen was released through Allihn-type fluid-cooled condenser connected to a bottle filled with water at room temperature. Then, H_2 was collected by replacing the water in a beaker. The volume of H_2 was normalized to the standard conditions (0 °C, 1 atm).

The measurements of viscosity of $NaBH_4$ solutions were performed using Ostwald viscometer. Temperature of the water bath was maintained constant with accuracy of 0.1 °C. Each experimental point has been measured at least 10 times and experimental errors were always below 2%. The initial $NaBH_4$ solution ([$NaBH_4]_0$ = 2 mol/ L, pH = 14) and the solution obtained after a completion of the hydrolysis experiment were used for the measurements.

3. Results and discussion

3.1. Dependence of the composition and morphology of Ni-Co-NPs from the synthesis conditions

The diffraction pattern of the obtained during the synthesis Ni-Co-NPs are presented in Fig. 1a. They show a presence of three broad peaks at around 2θ = 56.6, 66.3, and 101.7 º, which are attributed to the nano-sized metals. For the $Ni_{25}Co_{75}$ and $Ni_{50}Co_{50}$, a slight splitting of the peaks can be observed (Fig. 1b). This splitting indicates a two-phase composition of the powders comprising of Ni-rich and Co-rich particles. At the same time, an absence of additional peaks indicates the absence of impurities such as unreacted hydroxides or oxides of Ni and Co. The crystallite sizes for the synthesized materials were in a range 12–18 nm as derived by Scherer's equation [43].

Elemental analysis (EDS) showed that the compositions of the obtained products well agree with the Ni/Co ratios in the initial reaction mixtures (Table 1).
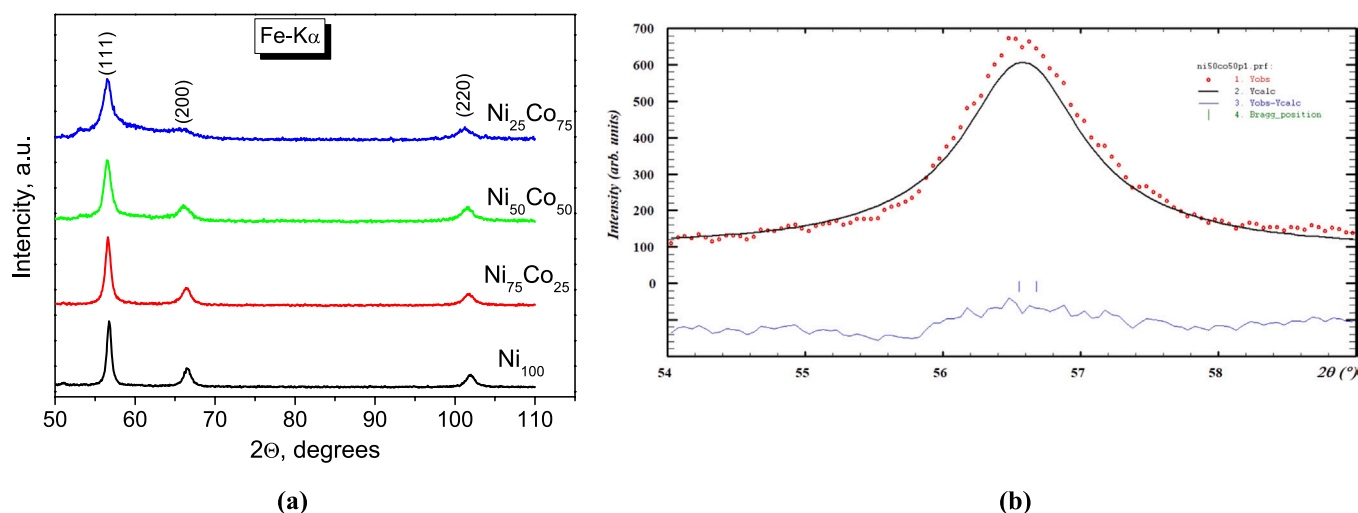
Fig. 1. XRD-pattern of Ni-Co-NPs (*a*) and splitting of the (111) peak for the Ni$_{50}$Co$_{50}$ sample (*b*).

Table 1
The size and composition of Ni-Co-NPs.

| Ni/Co ratio in the reaction mixture	Size of the particles, nm (from … to)	Content, weight %	
		Ni	Co
100/0	200 … 450	100	–
75/25	140 … 300	77	23
50/50	130 … 250	50.5	49.5
25/75[a]	80 … 200 (Ni-rich)	29	71
	0.5 … 2 µm (Co-rich)		

[a] The particles size ranges for the different fractions of Ni$_{25}$Co$_{75}$ (see Fig. 3) are given.

Using SEM characterization, we conclude that the size of the Ni-Co-NPs decreases with decreasing Ni fraction (until it reaches 50%) from ~250 nm for Ni$_{100}$ to ~150 nm for Ni$_{50}$Co$_{50}$. However, following a further decrease in the Ni content to Ni$_{25}$Co$_{75}$, the particles become larger, reaching 2 µm in maximum (Fig. 2). At the same time, for the obtained nanopowders the sizes of the crystallites evaluated by using Scherer's equation were 12–18 nm. Such a difference between the size of the crystallites and the particle sizes indicates that the nanoparticles formed contain crystallites of different sizes depending on the synthesis conditions. This phenomenon is typical for the chemically synthesized nanoparticles and was observed by the authors for the Ni and Ni-Cu nanoparticles earlier [44,45].

It was found that the large particles (Fig. 3, point 1) contained 25% Ni and 75% Co while the small ones (Fig. 3, point 2) contained 43% Ni and 57% Co. Thus, a multiphase mixture has been formed at high Co content.

3.2. Hydrolysis of NaBH₄ catalyzed by Ni-Co-NPs

The catalytic activity of Ni-Co-NPs as related to the Ni/Co ratios was investigated at various concentrations of NaBH$_4$, pH of the solutions and temperatures. It was found that in all the cases the hydrolysis process was complete as experimentally measured volumes of the released H$_2$ were equal to the theoretical, calculated using Eq. (1) value (2350 mL per 1 g NaBH$_4$).

$$NaBH_4 + 4\,H_2O \rightarrow NaB(OH)_4 + 4\,H_2\uparrow \qquad (1)$$
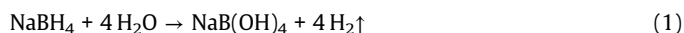
ΔH^0 = 250.5 kJ/mol [46,47].

This fact further to the completeness of the hydrolysis transformation of NaBH$_4$, shows an excellent efficiency of the catalysts.

Therefore, herein the kinetic curves of H$_2$ evolution are presented in terms "$V(H_2)_t/V(H_2)_{fin}$ vs *Time*". Furthermore, to compare the values of the H$_2$ evolution rate herein and those mentioned in the introductory section, these values are presented as: (1) in terms of "mL of H$_2$ per time per 1 g of catalyst" (ω, mL/min/g$_{cat}$); (2) in terms of "mL of H$_2$ per time per 1 g of catalyst per 1 g of NaBH$_4$" (υ, mL/min/g$_{cat}$/g$_{NaBH4}$), and (3) in terms of zero-order rate constant (k, mol/L/min/g$_{cat}$).

3.2.1. Dependence of the rate of H₂ evolution on the type of a catalyst

An influence of the composition of Ni-Co-NPs on the rate of hydrogen evolution during the hydrolysis of NaBH$_4$ was studied at pseudo-isothermal conditions at 25 °C for the following reactants mixtures: m(Ni-Co-NPs) = 0.3 g; pH = 9; [NaBH$_4$]$_0$ = 1 mol/L; volume of the solution = 5 mL.

It was found that in all cases the specific rates of H$_2$ generation are rather high and they increase with increasing Co content in Ni-Co-NPs (Table 2). The highest rate of H$_2$ evolution was observed for Ni$_{50}$Co$_{50}$ while an increase in Co content to 75% leads to a sharp decrease in the rate of the reaction. This may be caused by the change of the particles morphology. Indeed, Ni$_{25}$Co$_{75}$ nanopowders consist of two fractions – large and small particles (see Fig. 2, Table 1) which causes a decrease in the specific surface area of the catalyst. We note that a sharp decrease in the rate of H$_2$ evolution for Ni$_{25}$Co$_{75}$ is similar to the non-monotonous change in the rate of NaBH$_4$ hydrolysis with increasing Co content in the hydrogel-supported CoNi bimetallic alloys [48] (see Table 3 below) as well as in amorphous Ni-Co-B catalysts [16]. In [16] such changes were related to the highest content of boron in the most effective sample. We believe that a related mechanism of influence of the Ni-Co-NPs catalysis on the NaBH$_4$ hydrolysis is valid for the studied in the present study catalysts as well.

As it was mentioned in the Experimental Section, the Ni-Co-NPs were stored in water, and the surface of the particles was partially oxidized by the dissolved oxygen when a thin surface layer of Ni/Co hydroxides was formed. After addition of NaBH$_4$ solution to the catalysts, these hydroxides should be reduced to the nanoparticles of Ni-Co-B and then they can participate in the catalytic reaction. This assumption will be studied further in our future work.

At the same time, it must be noted that in all cases a linear time dependence of the volume of the released H$_2$ reaching up to ~95% of conversion of reaction was observed (Fig. 4). Thus, taking into account that
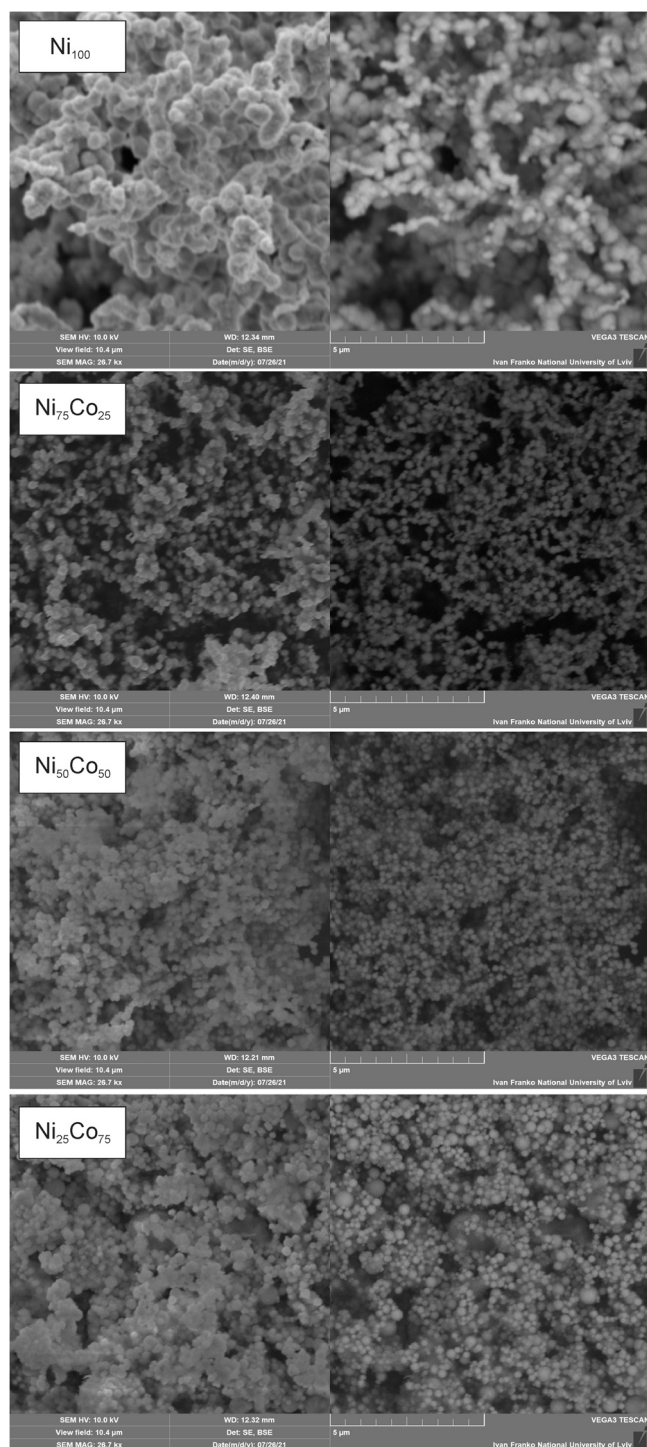
Fig. 2. SEM-images of Ni-Co-NPs with various Ni/Co ratios.

$$\frac{d(V(H_2)_t/V(H_2)_{fin})}{dt} = -\frac{d([NaBH_4]_t/[NaBH_4]_0)}{dt}$$

we can assume a zero-order reaction with respect to the concentration of NaBH$_4$:

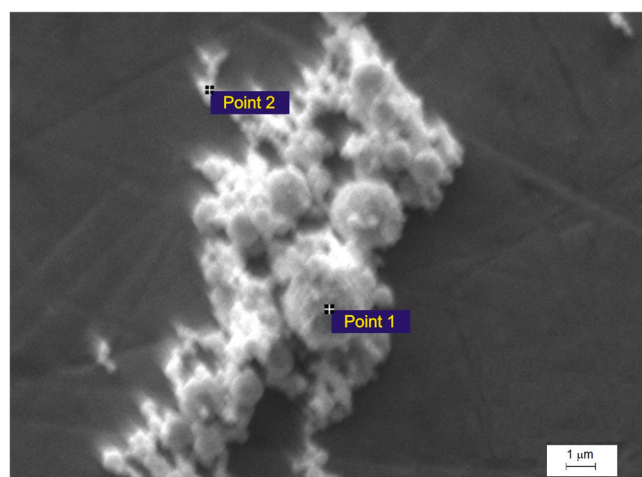$$-\frac{d([NaBH_4]_t)}{dt} = k$$

$$[NaBH_4]_t = [NaBH_4]_0 - kt \tag{2}$$

Fig. 3. SEM-image of Ni$_{25}$Co$_{75}$-NPs.

Table 2
Dependence of the specific rate of hydrogen evolution (υ) on the composition of a catalyst.

Catalyst	pH	[NaBH$_4$]$_0$, mol/L	ω, mL/ min/g$_{cat}$	υ, mL/min/ g$_{cat}$/g$_{NaBH4}$	k, mol/L/ min/g$_{cat}$
Ni$_{100}$	9	1	62	325	0.14
Ni$_{75}$Co$_{25}$			253	1330	0.56
Ni$_{50}$Co$_{50}$			295	1600	0.66
Ni$_{25}$Co$_{75}$			110	580	0.25

Table 3
Dependence of the specific rate of hydrogen evolution (υ) on the pH of the reaction mixture.

Catalyst	pH	[NaBH$_4$]$_0$, mol/L	ω, mL/ min/g$_{cat}$	υ, mL/min/ g$_{cat}$/g$_{NaBH4}$	k, mol/L/ min/g$_{cat}$
Ni$_{50}$Co$_{50}$	9	1	295	1600	0.66
	11		260	1400	0.58
	14		227	1200	0.50
NiNPs[a]	9	0.661	138	––	––
	10		136	––	––
	11		6	––	––
Co-Ni (0:5)[b]	13.87	0.53	10	––	––
Co-Ni (1:4)[b]			15	––	––
Co-Ni (2:3)[b]			30	––	––
Co-Ni (3:2)[b]			72	––	––
Co-Ni (4:1)[b]			68	––	––

[a] Notes. Reference data taken from [42], Table 3.
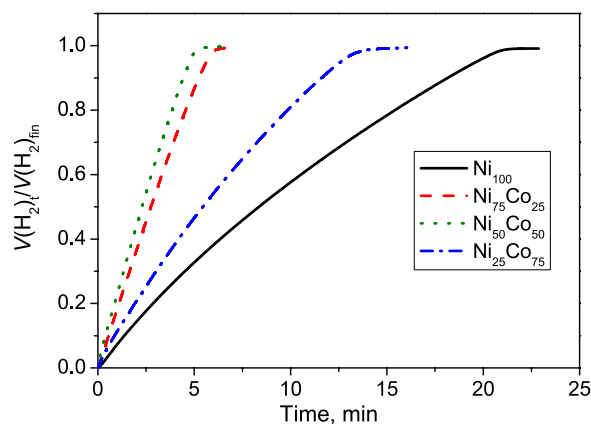[b] Reference data taken from [48], Fig. 4A.

Fig. 4. Kinetic curves of H$_2$ evolution measured in presence of Ni-Co-NPs.
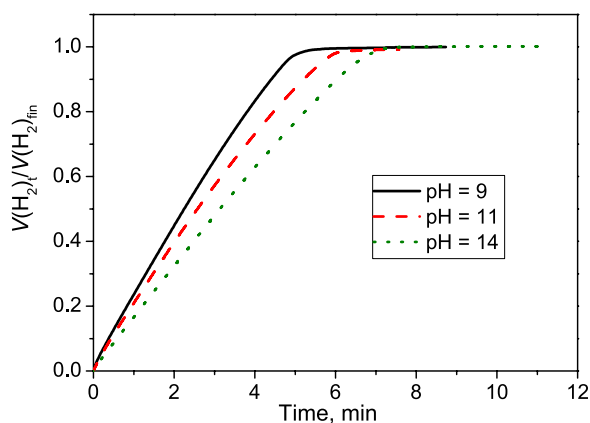
Fig. 5. Kinetic curves of H$_2$ evolution for various pH of the solutions, when catalyzed by Ni$_{50}$Co$_{50}$-NPs.

Due to the fact that the highest efficiency of catalysis was observed for Ni$_{50}$Co$_{50}$, the following experiments were carried out for this catalyzer.

3.2.2. An influence of pH on the hydrolysis of NaBH$_4$

The dependence of the kinetics of NaBH$_4$ hydrolysis on the pH of the reaction solution was studied at 25 °C for the following reactants mixtures: m(Ni$_{50}$Co$_{50}$) = 0.3 g; [NaBH$_4$]$_0$ = 1 mol/L; volume of the solution = 5 mL.

It appears that the rate of H$_2$ evolution only slightly depends on the concentration of OH$^-$ (Fig. 5). Indeed, an increase in the concentration of OH$^-$ in 10^5 times (from $1 \cdot 10^{-5}$ mol/L to 1 mol/L) leads to a decrease of the specific rate of the reaction by 25% only (Table 3). Such unexpectedly low dependence of the rate of NaBH$_4$ hydrolysis on pH assumes a zero order of the reaction with respect to [OH$^-$].

Furthermore, the rates of hydrogen evolution via the hydrolysis of NaBH$_4$ catalyzed by thermal plasma synthesized NiNPs [42] are listed in Table 3 for comparison. From Table 2, for the activity of the thermal plasma synthesized NiNPs is slightly higher than that for the chemically synthesized NiNPs studied in the present work. This can be related to the difference in the sizes of the particles and, respectively, in the specific surface area of the catalysts. However, the hydrolysis of NaBH$_4$ catalyzed by NiNPs is stopped at pH = 11, while, in contrast, it continues for Ni$_{50}$Co$_{50}$ thus showing advantages of the bimetallic catalysts. The rates of H$_2$ evolution in the presence of hydrogel supported Co-Ni nanoalloys presented in Table 3 show similar dependencies. Indeed, pure nickel shows the lowest efficiency as a catalyzer during the hydrolysis of NaBH$_4$.

3.2.3. An influence of NaBH$_4$ concentration on the kinetics of hydrolysis

The dependence of the kinetics of NaBH$_4$ hydrolysis on the initial concentration of sodium borohydride was studied at 25 °C for the following conditions: m(Ni$_{50}$Co$_{50}$) = 0.3 g; pH = 14; volume of the solution = 5 mL.

It was found that the rate of hydrogen evolution ω (and the corresponding rate constant k) increase with an increase of NaBH$_4$ concentration within the range of concentrations 0.1 – 1 mol/L but sharply decreased at [NaBH$_4$]$_0$ = 2 mol/L. It must be noted that the decrease in the rate of the hydrolysis reaction with increasing NaBH$_4$ concentration when it is higher than ~1 mol/L has been reported earlier [42,49], and was explained by the blocking of the surface of the catalyst by the formed metaborates [50] and/or formation of the hydrated macrostructures based on metaborates [51] causing an increased viscosity of the reaction solution.

Besides, the changes in the value of υ (Table 4) should be accounted as well. As it can be seen, the specific rate (υ) of H$_2$ evolution decreased with the increase in NaBH$_4$ concentration contrary to the

Table 4
Dependence of the specific rate and the rate constants of hydrogen evolution on the initial concentration of NaBH$_4$.

Catalyst	pH	[NaBH$_4$]$_0$, mol/L	ω, mL/min/g$_{cat}$	υ, mL/min/g$_{cat}$/g$_{NaBH4}$	k, mol/L/min/g$_{cat}$
Ni$_{50}$Co$_{50}$	14	0.1	89	4700	0.20
		0.5	147	1550	0.33
		1	277	1200	0.50
		2	123	320	0.27

values of ω and k. This increase in the specific rate of H$_2$ evolution is clearly observed from the Fig. 6a. The hydrolysis reaction was finished in ~2.5, ~5, ~8, and ~25 min for the concentrations of NaBH$_4$ of 0.1, 0.5, 1, and 2 mol/L, respectively. This feature can be related to the increase in the ratio "NaBH$_4$ / catalyst" and also this indicates that the rate of the process is diffusion-controlled.

Using the calculated values of the rate constants (which are equal to the rate of the hydrolysis, see Eq. (2)), we found that in the concentrations range from 0.1 to 1 mol/L the reaction order with respect to [NaBH$_4$] is close to 0.4 (Fig. 6b).

3.2.4. Activation parameters of the hydrolysis of NaBH$_4$ catalyzed by Ni$_{50}$Co$_{50}$

Analysis of the obtained experimental data (Sections 3.2.2 and 3.2.3) shows that their explanation is not straightforward. Indeed,

1) The kinetic curves of H$_2$ evolution are linear which indicates that a zero-order reaction with respect to [NaBH$_4$] is always the case.
2) The order of the reaction calculated using the dependence of the hydrolysis rate on the initial concentration of NaBH$_4$ with respect to [NaBH$_4$] is 0.4.

If the reaction order with respect to NaBH$_4$ is zero, then the process is controlled by the diffusion while its activation energy (E_A) must be low. However, many reference publications (see Introduction Section) on Ni-Co catalysts reported the that values of E_A are quite high exceeding 35 kJ/mol. The observed pseudo-zero-order kinetics of the reaction may be caused by different reasons. One possibility is an inability to achieve a required temperature stabilization of the reaction mixture. This is caused by a high value of the ΔH^0 of the hydrolysis reaction. Thus, at the applied conditions (5 mL of 1 mol/L NaBH$_4$ solution), the amount of generated heat (Q) is close to 1.25 kJ (Q = ΔH^0 ×V(solution)* [NaBH$_4$] = 250.5 kJ/mol× 0.005 L × 1 mol/L). Assuming adiabatic conditions of the interaction / absence of heat removal, the temperature of the reaction mixture should increase by $\Delta T = \frac{Q}{m \cdot c(H_2O)} \approx \frac{1.25}{0.005 \cdot 4.18} \approx 60$ (!) degrees. In such a case, a local overheating of the reaction system will necessarily occur. That is why we studied the temperature dependencies of the hydrolysis process at low concentrations of NaBH$_4$ and catalyst while using larger volumes of the reaction mixtures (Table 5, Fig. 7).

It was found that with decrease of the concentrations of NaBH$_4$ and Ni$_{50}$Co$_{50}$ and simultaneous increase of the volume of the reaction mixture, the activation energy decreased from 45 kJ/mol to 26 kJ/mol. Here it must be noted that the measured activation energy of NaBH$_4$ hydrolysis is quite low as compared to both noble and non-noble catalysts (Table 5). Such a fact shows a good promise for the future of chemically synthesized Ni-Co-NPs as catalysts for their use in the hydrogen evolution reactions.

Besides, the kinetic curves of hydrogen generations remain linear even for the lowest rates of the reactions (case (**III**) in Table 5, Fig. 7, a).

The linear kinetic curves (i.e., zero-order kinetics with respect to NaBH$_4$, Fig. 7a) of hydrogen evolution as well as low energy of activation of the hydrolysis process indicate that the rate of the
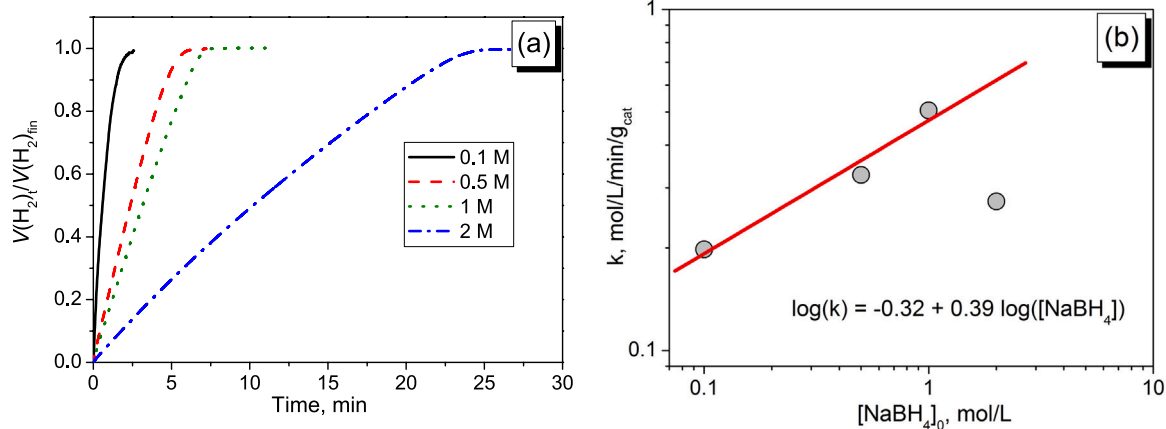
Fig. 6. Kinetic curves of H_2 evolution in presence of $Ni_{50}Co_{50}$ at various initial concentrations of $NaBH_4$ (a) and the dependence of the observable rate constants of the hydrolysis from the initial concentration of $NaBH_4$ (b).

Table 5
Temperature dependencies of the parameters of $NaBH_4$ hydrolysis reaction as related to the applied experimental conditions.

t, °C	k, mol/L/min/g_{cat}	Q, kJ	ΔT, °	E_A, kJ/mol
(I) $m(Ni_{50}Co_{50}) = 0.3$ g; $[NaBH_4]_0 = 0.1$ mol/L; $V(reaction\ mix) = 10$ mL; pH = 14				
25	0.093	0.25	6	45 ± 1
30	0.13			
40	0.24			
50	0.40			
60	0.65			
(II) $m(Ni_{50}Co_{50}) = 0.075$ g; $[NaBH_4]_0 = 0.025$ mol/L; $V(reaction\ mix) = 20$ mL; pH = 14				
25	0.13	0.125	1.5	38 ± 1
30	0.17			
42	0.32			
50	0.42			
60	0.65			
(III) $m(Ni_{50}Co_{50}) = 0.075$ g; $[NaBH_4]_0 = 0.01$ mol/L; $V(reaction\ mix) = 50$ mL; pH = 14				
25	0.025	0.125	0.6	26 ± 1
30	0.030			
40	0.044			
51	0.059			
60	0.074			
Co–Ni–P–B catalyst with the ratio Co/Co + Ni) = 0.85 (Ref. [19])		29		
Hydrogel supported Co-Ni nanoalloys (Ref. [48])		36.24		
Ru(0) nanoclusters (Ref. [52])		28.5		
Platinum nanoparticles (2–4 nm) (Ref. [53])		39.2		
Carbon nanotube supported platinum catalyst (Ref. [54])		27		

reaction is diffusion-controlled. Here it should be noted that zero-order reaction with respect to $[NaBH_4]$ was also observed for the Ru(0) catalyzed hydrolysis of sodium borohydride [52] and the low value of E_A (28.5 kJ/mol, see Table 5) was observed.

Hence, the temperature dependencies of the viscosity of the initial solutions and the solutions after the hydrolysis were studied. The values of enthalpy of activation of the viscous flow (ΔH_η) were calculated by using the Eq. (3):

$$\eta = A \exp\left(\frac{\Delta H_\eta}{RT}\right)$$

(3)

It was found (Fig. 8) that the enthalpy of activation of the viscous flow of the initial solution ($NaBH_4$ +NaOH) is quite low and equals to 12 kJ/mol and such a value is more than twice lower as compared to the E_A of the hydrolysis process.

However, the value of ΔH_η for the products of the reaction is much higher (~20 kJ/mol) and is comparable to the value of E_A of the hydrolysis of $NaBH_4$. Such a value of ΔH_η is slightly higher as compared to the one reported in [55] for the H_3BO_3 (~15 kJ/mol; this calculated value was obtained using the data presented in Fig. 6c [55]), but it must be noted that the enthalpies of activation of viscous flow depend on the composition of the solution [56]. Besides, in the above-mentioned References the values of pH were lower as compared to present study and, in addition, at high concentrations sodium metaborate formed via reaction (1) can transform into the
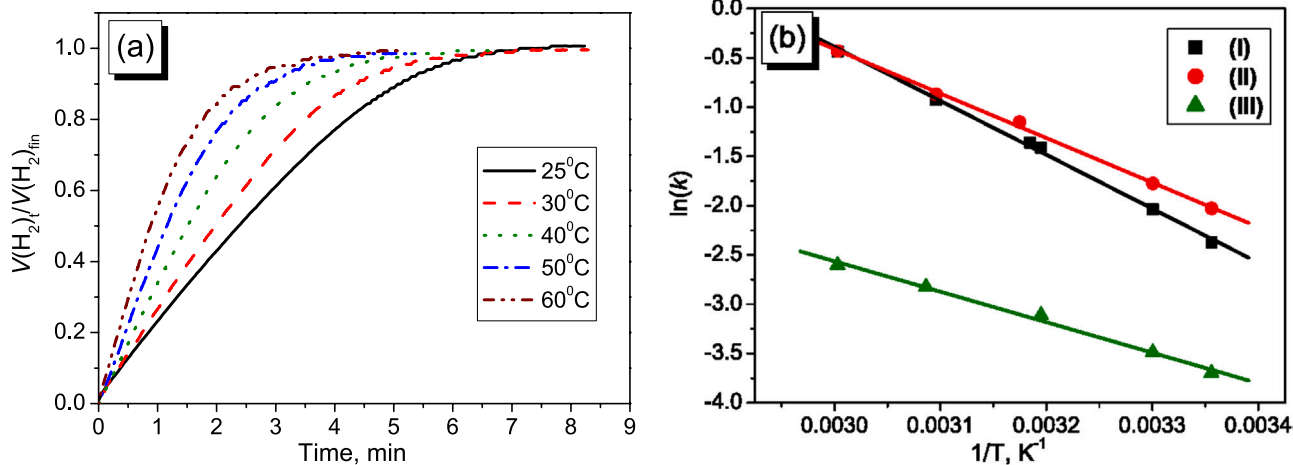

Fig. 7. Kinetic curves of hydrogen evolution at different temperatures (conditions of the reaction are the same as in the case (III) listed in Table 5) (a) and the temperature dependencies of the observable rate constants of $NaBH_4$ hydrolysis in the Arrhenius coordinates (b).
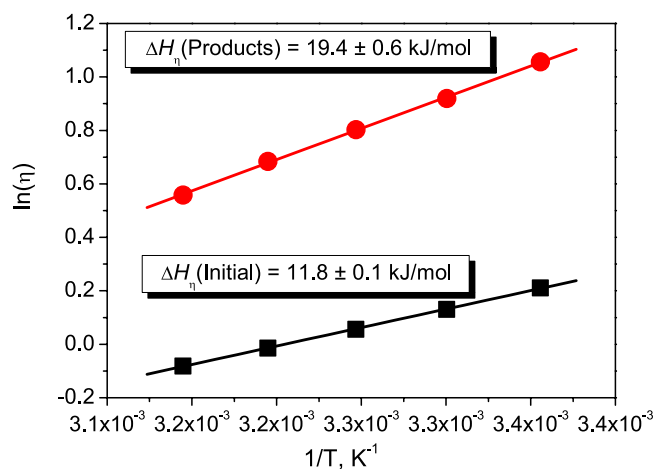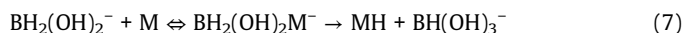
Fig. 8. The temperature dependencies of the viscosity of the initial solution and a solution after the hydrolysis was complete in coordinates of Eq. (3).

hydrated macrostructures [51], and this complicates the behavior of the solutions. Therefore, we assume that the enthalpy of activation of viscous flow of solutions obtained after a completion of the hydrolysis process is high. Nevertheless, more detailed future rheological studies of such solutions are required.

The metal-catalyzed $NaBH_4$ hydrolysis proceeds via the main stages described in the following Eqs. (4 – 9) [57]:

$$BH_4^- + M \Leftrightarrow BH_3M^- + MH \tag{4}$$

$$BH_3M^- + H_2O \rightarrow MH + BH_3(OH)^- \tag{5}$$

$$BH_3(OH)^- + M \Leftrightarrow BH_3(OH)M^- \rightarrow MH + BH_2(OH)_2^- \tag{6}$$

$$BH_2(OH)_2^- + M \Leftrightarrow BH_2(OH)_2M^- \rightarrow MH + BH(OH)_3^- \tag{7}$$

$$BH(OH)_3^- + M \Leftrightarrow BH(OH)_3M^- \rightarrow MH + B(OH)_4^- \tag{8}$$

$$2\,MH \rightarrow 2\,M + H_2 \tag{9}$$

Taking into account the well-known mechanism of interaction of hydrogen with Raney nickel in the reduction reactions [58], we assume that the elementary reactions of the hydrolysis of $NaBH_4$ catalyzed by Ni-based catalysts will be the same as that for Pd. As it can be seen, BH_4^- and intermediate $(BH_x(OH)_{4-x}^-)$ are first chemisorbed on the metal atoms subsequented by the dehydrogenation and formation of $B(OH)_4^-$ ions as a result. Thus, we can assume also that the rate of the reaction is controlled by the diffusion of $B(OH)_4^-$, i.e., by the rate of reactivation of the active centers of the catalyst making them available for the continuous BH_4^- ions chemisorption.

4. Conclusions

Ni-Co-NPs with various Ni/Co ratios were synthesized by modified polyol method via the reduction of Ni and Co hydroxide by hydrazine in water / ethylene glycol solutions. Using SEM it was found that the size and polydispersity of the obtained NPs slightly decrease with decreasing Ni content in the initial reaction mixture from 100% to 50%.

For $Ni_{25}Co_{75}$ catalyst, two fractions of the nanopowders were obtained and the particles with the size in a range 80 – 200 nm were found to be Ni-rich while the particles with the size ranging between 0.5 and 2 μm were concluded to be Co-rich.

Obtained Ni-Co-NPs were tested as catalysts of hydrogen generation via the hydrolysis of alkaline solutions of $NaBH_4$. We found that:

1) The most efficient catalyst of the hydrolysis reaction is $Ni_{50}Co_{50}$ providing the rate of H_2 evolution of 230 mL/min per 1 g of catalyst or 1200 mL/min per 1 g of catalyst per 1 g of $NaBH_4$;
2) The hydrolysis reaction catalyzed by $Ni_{50}Co_{50}$ is described by zero-order reaction kinetics with respect to the concentration of $NaBH_4$;
3) The activation energy of the process decreases with decreasing concentrations of $NaBH_4$ from 45 kJ/mol to 26 kJ/mol;
4) The rates of hydrogen evolution slightly depend on the pH decreasing by 25% only when pH of the solution increased from 9 to 14.

The enthalpy of activation of viscous flow of the initial $NaBH_4$ solution is 12 kJ/mol but the ΔH_η of the solution obtained after the completion of the hydrolysis is 20 kJ/mol.

Based on the obtained experimental data and calculations of the thermal effect of the hydrolysis reaction we conclude that.

a) The reaction is controlled by the diffusion of the formed at the surface of the catalyst $B(OH)_4^-$ ions;
b) The increase of E_A with increasing the concentrations of reagents may be caused by the local overheating causing the temperature fluctuations in the reaction mixture.

CRediT authorship contribution statement

A. Kytsya: Investigation, Formal analysis, Visualization, Writing – original draft, Writing – review & editing. **V. Berezovets**: Investigation, Formal analysis, Visualization, Writing – original draft, Writing – review & editing. **Yu. Verbovytskyy**: Investigation, Formal analysis, Visualization, Writing – original draft, Writing – review & editing. **L. Bazylyak**: Investigation, Formal analysis, Visualization, Writing – original draft, Writing – review & editing. **V. Kordan**: Investigation, Formal analysis, Visualization, Writing – original draft, Writing – review & editing. **I. Zavaliy**: Conceptualization, Supervision, Writing – review & editing, Project administration, Funding acquisition. **V.A. Yartys**: Conceptualization, Supervision, Writing – review & editing, Project administration, Funding acquisition.

Declaration of Competing Interest

The authors declare that they have no known competing financial interests or personal relationships that could have appeared to influence the work reported in this paper.

References

[1] L. Ouyang, W. Chen, J. Liu, M. Felderhoff, H. Wang, M. Zhu, Enhancing the regeneration process of consumed $NaBH_4$ for hydrogen storage, Adv. Energy Mater. 1700299 (2017) 1–8, https://doi.org/10.1002/aenm.201700299

[2] K. Chen, L. Ouyang, H. Zhong, J. Liu, H. Wang, H. Shao, Y. Zhang, M. Zhu, Converting H+ from coordinated water into H− enables super facile synthesis of $LiBH_4$, Green Chem. 21 (2019) 4380–4387, https://doi.org/10.1039/C9GC01897B

[3] V. Yartys, I. Zavaliy, Yu. Pirskyy, Yu. Solonin, V. Berezovets, F. Manilevich, Yu. Verbovytskyy, A. Kytsya, A. Kutsyi, Hydrogen generation by hydrolysis of metals and hydrides for portable energy supply, in: V. Yartys, Yu Solonin, I. Zavaliy (Eds.), Hydrogen Based Energy Storage: Status and Recent Developments, Publishing Office "Prostir-M", Lviv, 2021, pp. 15–37.

[4] B.H. Liu, Z.P. Li, A review: hydrogen generation from borohydride hydrolysis reaction, J. Power Sources 187 (2) (2009) 527–534, https://doi.org/10.1016/j.jpowsour.2008.11.032

[5] U.B. Demirci, O. Akdim, J. Andrieux, J. Hannauer, R. Chamoun, P. Miele, Sodium borohydride hydrolysis as hydrogen generator: issues, state of the art and applicability upstream from a fuel cell, Fuel Cells 10 (3) (2010) 335–350, https://doi.org/10.1002/fuce.200800171

[6] S.S. Muir, X. Yao, Progress in sodium borohydride as a hydrogen storage material: development of hydrolysis catalysts and reaction systems, Int. J. Hydrog. Energy 36 (10) (2011) 5983–5997, https://doi.org/10.1016/j.ijhydene.2011.02.032

[7] R. Retnamma, A.Q. Novais, C.M. Rangel, Kinetics of hydrolysis of sodium borohydride for hydrogen production in fuel cell applications: a review, Int. J. Hydrog. Energy 36 (16) (2011) 9772–9790, https://doi.org/10.1016/j.ijhydene.2011.04.223

[8] V.I. Simagina, O.V. Netskina, O.V. Komova, A.M. Ozerova, Progress in the catalysts for H₂ generation from NaBH₄ fuel, Curr. Top. Catal. 10 (2012) 147–165.

[9] U.B. Demirci, The hydrogen cycle with the hydrolysis of sodium borohydride: a statistical approach for highlighting the scientific/technical issues to prioritize in the field, Int. J. Hydrog. Energy 40 (2015) 2673–2691, https://doi.org/10.1016/j.ijhydene.2014.12.067

[10] J.A. Adeniran, J.J. de Koker, E.T. Akinlabi, T.C. Jen, Sustainable hydrogen generation substrates, catalysts and methods: an overview, in: 8th International Conference on Mechanical and, Intelligent Manufacturing Technologies (ICMIMT) (2017) 21–26, https://doi.org/10.1109/ICMIMT.2017.7917428.

[11] H. Sun, J. Meng, L. Jiao, F. Cheng, J. Chen, A review of transition-metal boride/phosphidebased materials for catalytic hydrogen generation from hydrolysis of boron-hydrides, Inorg. Chem. Front. 5 (2018) 760–772, https://doi.org/10.1039/C8QI00044A

[12] H.N. Abdelhamid, A review on hydrogen generation from the hydrolysis of sodium borohydride, Int. J. Hydrog. Energy 46 (2021) 726–765, https://doi.org/10.1016/j.ijhydene.2020.09.186

[13] J. Kim, H. Lee, S. Han, H. Kim, M. Song, J. Lee, Production of hydrogen from sodium borohydride in alkaline solution: development of catalyst with high performance, Int. J. Hydrog. Energy 29 (2004) 263–267, https://doi.org/10.1016/S0360-3199(03)00128-9

[14] B.H. Liu, Z.P. Li, S. Suda, Nickel- and cobalt-based catalysts for hydrogen generation by hydrolysis of borohydride, J. Alloy. Compd. 415 (2006) 288–293, https://doi.org/10.1016/j.jallcom.2005.08.019

[15] J.C. Ingersoll, N. Mani, J.C. Thenmozhiyal, A. Muthaiah, Catalytic hydrolysis of sodium borohydride by a novel nickel-cobaltboride catalyst, J. Power Sources 173 (2007) 450–457, https://doi.org/10.1016/j.jpowsour.2007.04.040

[16] R. Fernandes, N. Patel, A. Miotello, M. Filippi, Studies on catalytic behavior of Co-Ni-B in hydrogen production by hydrolysis of NaBH₄, J. Mol. Catal. A Chem. 298 (2009) 1–6, https://doi.org/10.1016/j.molcata.2008.09.014

[17] D. Kim, K. Cho, Y. Choi, C. Park, Fabrication of porous Co-Ni-P catalysts by electrodeposition and their catalytic characteristics for the generation of hydrogen from an alkaline NaBH₄ solution, Int. J. Hydrog. Energy 34 (2009) 2622–2630, https://doi.org/10.1016/j.ijhydene.2008.12.097

[18] R. Fernandes, N. Patel, A. Miotello, Efficient catalytic properties of Co-Ni-P-B catalyst powders for hydrogen generation by hydrolysis of alkaline solution of NaBH₄, Int. J. Hydrog. Energy 34 (2009) 2893–2900, https://doi.org/10.1016/j.ijhydene.2009.02.007

[19] N. Patel, R. Fernandes, A. Miotello, Promoting effect of transition metal-doped Co-B alloy catalysts for hydrogen production by hydrolysis of alkaline NaBH₄ solution, J. Catal. 271 (2010) 315–324, https://doi.org/10.1016/j.jcat.2010.02.014

[20] D. Park, T. Kim, Hydrogen generation from NaBH₄ hydrolysis on Co-Ni-P-B/Ni foam catalyst, Trans. Korean Hydrog. New Energy Soc. 21 (2010) 383–389.

[21] L. Li, Y. Wang, Y. Wang, Q. Ren, L. Jiao, H. Yuan, Effect of Ni content in Co₁₋ₓNiₓB catalysts on hydrogen generation during hydrolysis, Acta Phys. Chim. Sin. 26 (6) (2010) 1575–1578.

[22] C. Wu, Y. Bai, D.X. Liu, F. Wu, M.L. Pang, B.L. Yi, Ni-Co-B catalyst promoted hydrogen generation by hydrolyzing NaBH₄ solution for in situ hydrogen supply of portable fuel cells, Catal. Today 170 (2011) 33–39, https://doi.org/10.1016/j.cattod.2011.01.046

[23] M. Rakap, E.E. Kalu, S. Özkar, Cobalt-nickel-phosphorus supported on Pd-activated TiO₂ (Co-Ni-P/Pd-TiO₂) as cost-effective and reusable catalyst for hydrogen generation from hydrolysis of alkaline sodium borohydride solution, J. Alloy. Compd. 509 (2011) 7016–7021, https://doi.org/10.1016/j.jallcom.2011.04.023

[24] Y.P. Guo, Q.H. Feng, J.T. Ma, The hydrogen generation from alkaline NaBH₄ solution by using electroplated amorphous Co-Ni-P film catalysts, Appl. Surf. Sci. 273 (2013) 253–256, https://doi.org/10.1016/j.apsusc.2013.02.025

[25] G.Y. Hristov, E.Y. Chorbadzhiyska, R.S. Rashkov, Y.V. Hubenova, M.Y. Mitov, Comparison investigation of Co-based catalysts for the catalytic hydrolysis of sodium borohydride, Bulg. Chem. Commun. 45 (SI A) (2013) 219–222.

[26] Z. Li, H. Li, L. Wang, T. Liu, T. Zhang, G. Wang, G. Xie, Hydrogen generation from catalytic hydrolysis of sodium borohydride solution using supported amorphous alloy catalysts (Ni-Co-P/γ-Al₂O₃), Int. J. Hydrog. Energy 39 (27) (2014) 14935–14941, https://doi.org/10.1016/j.ijhydene.2014.07.063

[27] C.C. Chou, C.H. Hsieh, B.H. Chen, Hydrogen generation from catalytic hydrolysis of sodium borohydride using bimetallic Ni-Co nanoparticles on reduced graphene oxide as catalysts, Energy 90 (2015) 1973–1982, https://doi.org/10.1016/j.energy.2015.07.023

[28] L. Wang, Z. Li, P. Zhang, G. Wang, G. Xie, Hydrogen generation from alkaline NaBH₄ solution using Co-Ni-Mo-P/γ-Al₂O₃ catalysts, Int. J. Hydrog. Energy 41 (2016) 1468–1476, https://doi.org/10.1016/j.ijhydene.2015.11.028

[29] Y. Wei, W. Meng, Y. Wang, Y. Gao, K. Qi, K. Zhang, Fast hydrogen generation from NaBH₄ hydrolysis catalyzed by nanostructured Co-Ni-B catalysts, Int. J. Hydrog. Energy 42 (2017) 6072–6079, https://doi.org/10.1016/j.ijhydene.2016.11.134

[30] L. Wang, Z. Li, Y. Zhang, T. Zhang, G. Xie, Hydrogen generation from alkaline NaBH₄ solution using electroless-deposited Co-Ni-W-P/γ-Al₂O₃ as catalysts, J. Alloy. Compd. 702 (2017) 649–658, https://doi.org/10.1016/j.jallcom.2017.01.295

[31] K. Li, M. Ma, L. Xie, Y. Yao, R. Kong, G. Du, A.M. Asiri, X. Sun, Monolithically integrated NiCoP nanosheet array on Ti mesh: an efficient and reusable catalyst in NaBH₄ alkaline media toward on-demand hydrogen generation, Int. J. Hydrog. Energy 42 (2017) 19028–19034, https://doi.org/10.1016/j.ijhydene.2017.06.092

[32] A. Didehban, M. Zabihi, J. Rahbar Shahrouzi, Experimental studies on the catalytic behavior of alloy and core-shell supported Co-Ni bimetallic nano-catalysts for hydrogen generation by hydrolysis of sodium borohydride, Int. J. Hydrog. Energy 43 (2018) 20645–20660, https://doi.org/10.1016/j.ijhydene.2018.09.127

[33] J. Guo, Y. Hou, B. Li, Y. Liu, Novel Ni-Co-B hollow nanospheres promote hydrogen generation from the hydrolysis of sodium borohydride, Int. J. Hydrog. Energy 43 (2018) 15245–15254, https://doi.org/10.1016/j.ijhydene.2018.06.117

[34] A.M. Pornea, M.W. Abebe, H. Kim, Ternary NiCoP urchin like 3D nanostructure supported on nickel foam as a catalyst for hydrogen generation of alkaline NaBH₄, Chem. Phys. 516 (2019) 152–159, https://doi.org/10.1016/j.chemphys.2018.08.044

[35] J. Guo, B. Wang, D. Yang, Z. Wan, P. Yan, J. Tian, T.T. Isimjan, X. Yang, Rugae-like Ni₂P-CoP nanoarrays as a bi-functional catalyst for hydrogen generation: NaBH₄ hydrolysis and water reduction, Appl. Catal. B Environ. 265 (2020) 118584, https://doi.org/10.1016/j.apcatb.2019.118584

[36] M. Soltani, M. Zabihi, Hydrogen generation by catalytic hydrolysis of sodium borohydride using the nano-bimetallic catalysts supported on the core-shell magnetic nanocomposite of activated carbon, Int. J. Hydrog. Energy 45 (2020) 12331–12346, https://doi.org/10.1016/j.ijhydene.2020.02.203

[37] A. Paksoy, S.F. Kurtoğlu, A.K. Dizaji, Z. Altıntaş, S. Khoshsima, A. Uzun, Ö. Balcı, Nanocrystalline cobalt-nickel-boron (metal boride) catalysts for efficient hydrogen production from the hydrolysis of sodium borohydride, Int. J. Hydrog. Energy 46 (2021) 7974–7988, https://doi.org/10.1016/j.ijhydene.2020.12.017

[38] Y. Lee, A. Badakhsh, D. Min, Y.S. Jo, H. Sohn, C.W. Yoon, H. Jeong, Y. Kim, K. Kim, S.W. Nam, Development of 3D open-cell structured Co-Ni catalysts by pulsed electrodeposition for hydrolysis of sodium borohydride, Appl. Surf. Sci. 554 (1–11) (2021) 149530, https://doi.org/10.1016/j.apsusc.2021.149530

[39] O.V. Netskina, E.S. Tayban, V.A. Rogov, A.M. Ozerova, S.A. Mukha, V.I. Simagina, O.V. Komova, Solid-state NaBH4 composites for hydrogen generation: catalytic activity of nickel and cobalt catalysts, Int. J. Hydrog. Energy 46 (2021) 5459–5471, https://doi.org/10.1016/j.ijhydene.2020.11.078

[40] H.M. Rietveld, A profile refinement method for nuclear and magnetic structures, J. Appl. Crystallogr. 2 (2) (1969) 65–71, https://doi.org/10.1107/S0021889869006558

[41] L. Ouyang, M. Ma, M. Huang, R. Duan, H. Wang, L. Sun, M. Zhu, Enhanced hydrogen generation properties of MgH2-based hydrides by breaking the magnesium hydroxide passivation layer, Energies 8 (5) (2015) 4237–4252, https://doi.org/10.3390/en8054237

[42] N.P. Ghodke, S. Rayaprol, S.V. Bhoraskar, V.L. Mathe, Catalytic hydrolysis of sodium borohydride solution for hydrogen production using thermal plasma synthesized nickel nanoparticles, Int. J. Hydrog. Energy 45 (33) (2020) 16591–16605, https://doi.org/10.1016/j.ijhydene.2020.04.143

[43] A. Monshi, M.R. Foroughi, M.R. Monshi, Modified Scherrer equation to estimate more accurately nano-crystallite size using XRD, World J. Nano Sci. Eng. 2 (3) (2012) 154–160, https://doi.org/10.4236/wjnse.2012.23020

[44] I.Y. Zavaliy, A.R. Kytsya, Y.V. Verbovytskyy, Y.O. Kulyk, P.Y. Zavalij, Synthesis and structure of Ni-based nanopowders, in: 2018 IEEE 8th International Conference Nanomaterials: Application & Properties (NAP), IEEE, 2018, pp. 1:01SPN32-1 – 01SPN32-4, https://doi.org/10.1109/NAP.2018.8914926

[45] A.R. Kytsya, L.I. Bazylyak, I.Y. Zavaliy, Y.V. Verbovytskyy, P. Zavalij, Synthesis, structure and hydrogenation properties of Ni-Cu bimetallic nanoparticles, Appl. Nanosci. (2021), https://doi.org/10.1007/s13204-021-01742-6

[46] A. Garron, D. Świerczyński, S. Bennici, A. Auroux, New insights into the mechanism of H₂ generation through NaBH₄ hydrolysis on Co-based nanocatalysts studied by differential reaction calorimetry, Int. J. Hydrog. Energy 34 (3) (2009) 1185–1199, https://doi.org/10.1016/j.ijhydene.2008.11.027

[47] D.R. Lide, CRC Handbook of Chemistry and Physics, 82nd ed, CRC Press, Boca Raton, 2001.

[48] S. Chairam, P. Jarujamrus, M. Amatatongchai, Enhanced catalytic activity in hydrogen production from hydrolysis of sodium borohydride using starch hydrogel-CoNi bimetallic alloys, J. Iran. Chem. Soc. 18 (3) (2021) 689–699, https://doi.org/10.1007/s13738-020-02056-0

[49] Q. Zhang, Y. Wu, X. Sun, J. Ortega, Kinetics of catalytic hydrolysis of stabilized sodium borohydride solutions, Ind. Eng. Chem. Res. 46 (4) (2007) 1120–1124, https://doi.org/10.1021/ie061086t

[50] Y. Shang, R. Chen, Hydrogen storage via the hydrolysis of NaBH4 basic solution: optimization of NaBH₄ concentration, Energy Fuels 20 (5) (2006) 2142–2148, https://doi.org/10.1021/ef050363q

[51] Y. Zhou, S. Higa, C. Fang, Y. Fang, W. Zhang, T. Yamaguchi, B(OH)₄⁻ hydration and association in sodium metaborate solutions by X-ray diffraction and empirical

potential structure refinement, Phys. Chem. Chem. Phys. 19 (40) (2017) 27878–27887, https://doi.org/10.1039/C7CP05107G

[52] S. Özkar, M. Zahmakıran, Hydrogen generation from hydrolysis of sodium borohydride using Ru(0) nanoclusters as catalyst, J. Alloy. Compd. 404 (2005) 728–731, https://doi.org/10.1016/j.jallcom.2004.10.084

[53] C. Huff, E. Biehler, Q. Quach, J.M. Long, T.M. Abdel-Fattah, Synthesis of highly dispersive platinum nanoparticles and their application in a hydrogen generation reaction, Colloids Surf. A Physicochem. Eng. 610 (2021) 125734, https://doi.org/10.1016/j.colsurfa.2020.125734

[54] A. Uzundurukan, Y. Devrim, Hydrogen generation from sodium borohydride hydrolysis by multi-walled carbon nanotube supported platinum catalyst: a kinetic study, Int. J. Hydrog. Energy 44 (33) (2019) 17586–17594, https://doi.org/10.1016/j.ijhydene.2019.04.188

[55] Y.A. Hassan, S. Osturk, S. Lee, Rheological characterization of buffered boric acid aqueous solutions in light water reactors, Prog. Nucl. Energy 85 (2015) 239–253, https://doi.org/10.1016/j.pnucene.2015.06.025

[56] N.D. Solov'yova, I.I. Frolova, D.A. Legkaya, Physicochemical properties of low-component nickel-plating electrolyte, Condens. Matter Interphases 16 (2) (2014) 201–205.

[57] G. Guella, C. Zanchetta, B. Patton, A. Miotello, New insights on the mechanism of palladium-catalyzed hydrolysis of sodium borohydride from ^{11}B NMR measurements, J. Phys. Chem. B 110 (34) (2006) 17024–17033, https://doi.org/10.1021/jp063362n

[58] I. Horiuti, M. Polanyi, Exchange reactions of hydrogen on metallic catalysts, Trans. Faraday Soc. 30 (1934) 1164–1172, https://doi.org/10.1039/TF9343001164